THE JOURNAL OF PHYSICAL CHEMISTRY B

Article

Cite This: J. Phys. Chem. B 2017, 121, 9548-9556

pubs.acs.org/JPCB

Discrete-State Kinetics Model for NMR-Based Analysis of Protein Translocation on DNA at Equilibrium

Debashish Sahu and Junji Iwahara*

Department of Biochemistry and Molecular Biology, Sealy Center for Structural Biology and Molecular Biophysics, University of Texas Medical Branch, Galveston, Texas 77555-1068, United States

Supporting Information

ABSTRACT: In the target DNA search process, sequence-specific DNA-binding proteins first nonspecifically bind to DNA and stochastically move from one site to another before reaching their targets. To rigorously assess how the translocation process influences NMR signals from proteins interacting with nonspecific DNA, we incorporated a discrete-state kinetic model for protein translocation on DNA into the McConnell equation. Using this equation, we simulated line shapes of NMR signals from proteins undergoing translocations on DNA through sliding, dissociation/reassociation, and intersegment transfer. Through this analysis, we validated an existing NMR approach for kinetic investigations of protein translocation on DNA, which utilizes NMR line shapes of two nonspecific DNA−protein complexes and their mixture. We found that, despite its use of simplistic two-state approximation neglecting the presence of many microscopic states, the previously proposed NMR approach provides accurate kinetic information on the intermolecular translocations of proteins between two DNA molecules. Interestingly, our results suggest that the same NMR approach can also provide qualitative information about the one-dimensional diffusion coefficient for proteins sliding on DNA.

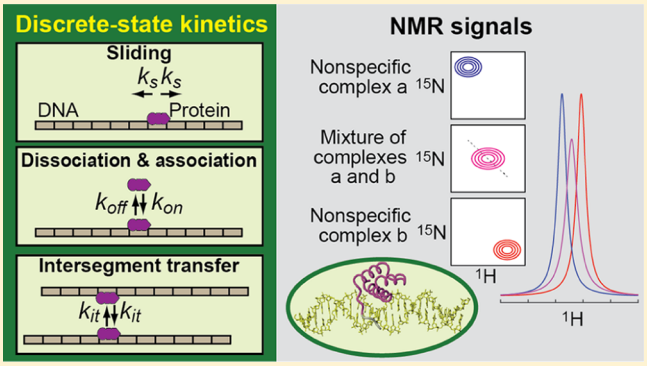

INTRODUCTION

To perform their functions, sequence-specific DNA-binding proteins, such as transcription factors must first locate their targets in the presence of enormous amounts of nonspecific DNA sequences. In the target search process, these proteins scan DNA through nonspecific interactions and move from one site to another on the DNA. Three major mechanisms for the translocation of proteins on DNA are known: (1) sliding, (2) dissociation and reassociation, and (3) intersegment transfer.[1−5] Sliding is the random walking of proteins while being nonspecifically bound to DNA. This movement is regarded as one-dimensional diffusion along the DNA. Translocation via dissociation and reassociation is often called hopping when this occurs in a short range between nearby sites. Intersegment transfer is the direct transfer of protein from one DNA duplex to another without going through the intermediary of free protein and occurs when two DNA duplexes are close enough for a DNA-bound protein molecule to transiently bridge the two DNA duplexes.

NMR spectroscopy has provided atomic-level insights into how proteins undergo translocation on nonspecific DNA in the target search process (e.g., reviewed in ref 6). Using NMR, structural details of the nonspecific protein−DNA interactions in solution were revealed for the lac repressor,[7] HoxD9,[8] Egr-1,[9,10] ZNF217,[11] ETV6,[12] and Ets-1.[13] One of the most important findings in these studies is that the nonspecific protein−DNA interactions are dynamic but share many structural features with the corresponding specific DNA complexes in terms of their electrostatic interactions with DNA backbone.

Among various spectroscopic techniques for analyzing molecular ensembles in solution, NMR spectroscopy is unique in that it can allow for investigating fast kinetics of various processes even at equilibrium. However, although NMR studies have provided structural insights into the dynamic, nonspecific DNA complexes of proteins, it remains challenging to analyze the kinetics of protein translocation on nonspecific DNA by NMR. Only a few papers have reported such NMR-based kinetic analyses of protein translocation on nonspecific DNA.[8,10,14] The difficulty in the kinetic analysis arises mainly from two issues. First, the simultaneous presence of multiple mechanisms makes it difficult to extract kinetic information on a particular mechanism for translocation. Second, the kinetic models commonly used for protein translocation on DNA are not necessarily suited to be integrated with NMR theory. In particular, the continuum model, which assumes a continuous distribution of proteins sliding along DNA as originally proposed in the field,[15] is unsuitable to incorporate into the

Received: August 4, 2017
Revised: September 15, 2017
Published: September 19, 2017

DOI: 10.1021/acs.jpcb.7b07779
J. Phys. Chem. B 2017, 121, 9548−9556

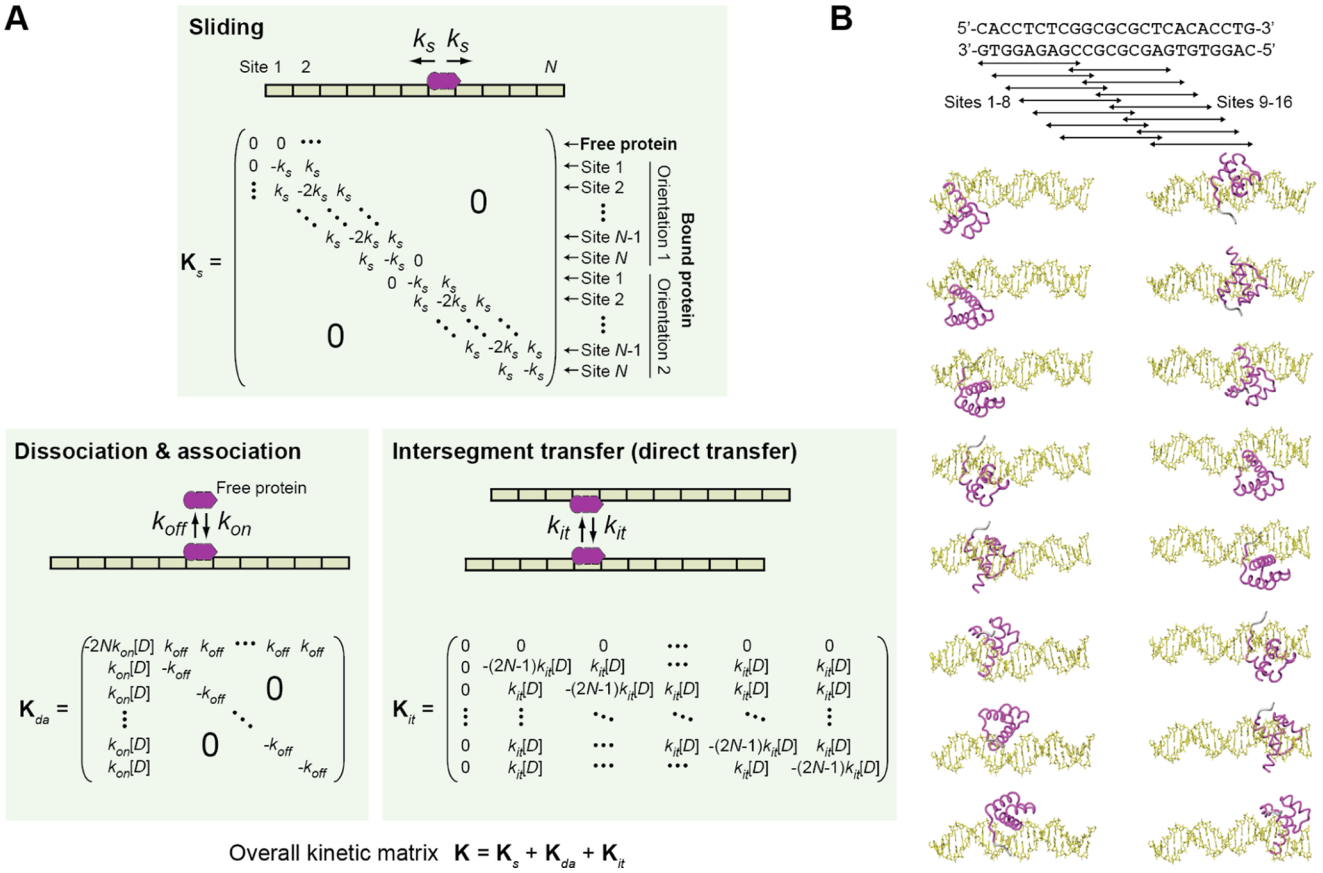

Figure 1. Discrete-state kinetics model for translocations of a protein interacting with DNA nonspecifically. (A) Kinetic matrices that describe sliding, dissociation/association, and intersegment transfer are shown for a system involving a DNA duplex with N sites and a protein. It is assumed that each nonspecific site exhibits the same kinetic properties. For each site, two opposite orientations of binding are possible due to the pseudo-C_2 symmetry of the DNA. The kinetic rate constants k_s, k_{off}, k_{on}, and k_{it} are defined as microscopic (as opposed to macroscopic) rate constants for each site. The macroscopic one-dimensional diffusion coefficient for sliding is given by eq 1. The macroscopic association rate constants for association, dissociation, and intersegment transfer are given by $2Nk_{on}$, k_{off}, and $2Nk_{it}$, respectively. [D] represents the concentration of DNA in the free state. Each matrix is a square matrix with a dimensionality of $2N + 1$, which corresponds to the total number of states of the protein (including the free state). Matrices for a system involving a protein and two DNA duplexes (as used in the mixture approach) are shown in the Supporting Information. These matrices are used in eqs 2−4. (B) Discrete states of nonspecific binding of a homeodomain protein to a 24 bp DNA. In this case, the protein covers 9 bp in each state and 16 sites ($N = 24 - 9 + 1$) are involved.

master equations of NMR spectroscopy. This is because defining NMR parameters as continuous functions of the position of protein with respect to DNA is virtually impossible.

Recent theoretical studies on target DNA search by proteins show that a discrete-state kinetic model, which assumes transitions between distinct adjacent nonspecific sites on DNA, can describe sliding and other translocation mechanisms more appropriately than the continuum model.[16−18] This type of discrete-state model has led to success in the kinetic analysis of protein translocation on DNA by fluorescence spectroscopy.[19,20] Fortunately, the discrete-state kinetic model is well suited for use with the NMR theory on chemical exchange.

In our current study, we incorporate the discrete-state kinetic model of protein translocation on DNA into the McConnell equation that describes the behavior of nuclear magnetization for an arbitrary number of exchanging states.[21,22] By solving these equations numerically, we rigorously analyze how the translocation process influences NMR signals from proteins that are nonspecifically bound to DNA. Through this analysis, we will validate an existing NMR approach for the kinetic investigations of protein translocations on nonspecific DNA at equilibrium and explore the extent of the kinetic information that can be obtained using the NMR approach.

EXPERIMENTAL AND THEORETICAL METHODS

In this section, we first present a discrete-state kinetic model describing protein translocation on nonspecific DNA and incorporate it into the McConnell equation. Then, we summarize the NMR approach that was previously proposed to analyze the kinetics of protein translocation on DNA, which we will theoretically assess.

Discrete-State Kinetics Model for Protein Translocation on DNA. In the present work, we adopt a discrete-state kinetic model for protein translocation on DNA,[17,19,20] which is schematically depicted in Figure 1A. This kinetic model assumes that a nonspecific DNA duplex contains N distinct sites for binding. For example, for 24 bp DNA and a protein that covers 9 bp at each site, N is calculated to be 16 (=24 − 9 + 1). Due to the structural pseudo-C_2 symmetry of each DNA site, two opposite orientations are possible for a protein to bind to each site through short-range electrostatic interactions with the DNA backbone. Each nonspecific site is assumed to exhibit the same kinetic properties with the same

DOI: 10.1021/acs.jpcb.7b07779
J. Phys. Chem. B 2017, 121, 9548−9556

rate constants for sliding (k_s), dissociation (k_{off}), association (k_{on}), and intersegment transfer (k_{it}). These kinetic rate constants are microscopic rate constants defined for each sites (not for the entire DNA molecule). The macroscopic association rate constant for the DNA duplex is given by $2Nk_{on}$ and thus $k_{off}/(2Nk_{on})$ corresponds to the macroscopic apparent dissociation constant ($K_{d,app}$). As previously described,[19] the sliding rate constant k_s is directly related to the macroscopic one-dimensional diffusion coefficient for sliding (D_1) as follows

$$D_1 = l^2 k_s \tag{1}$$

where l represents the distance (3.4 Å) between adjacent sites along the DNA axis. As previously noted, D_1 given in units of $bp^2\ s^{-1}$ is equivalent to k_s.[19] Because the NMR experiments typically use DNA duplexes shorter than the persistence length (i.e., ~150 bp), intersegment transfers within the same DNA duplex are neglected and only those between two DNA duplexes are considered. For this type of intermolecular intersegment transfer, the k_{it} constant is a second-order rate constant, as previously described.[19,20] When the NMR experiments are conducted for solutions in which the concentration of each component typically remains constant due to equilibrium (in terms of chemical species), any second-order processes can be considered with a pseudo-first-order treatment, enabling the use of a kinetic matrix even for second-order processes (see below). In a system containing a protein and a nonspecific DNA duplex, the total number of states of the protein, including the free state, is $2N + 1$. For a system containing a protein and two nonspecific DNA duplexes of the same length (e.g., the case for the mixture approach), this number is $4N + 1$. So, kinetic matrices with a dimensionality of either $2N + 1$ or $4N + 1$ are used in our current study.

Incorporation into the McConnell Equation. The discrete-state kinetic model for protein translocation on DNA is well suited to being incorporated into the McConnell equation for chemical exchange. The transverse magnetizations of discrete states can be represented by a column vector $\mathbf{m}$, in which each element corresponds to the transverse magnetization as a complex quantity, $m_n = m_{x,n} + im_{y,n}$, where i is the imaginary unit and $m_{x,n}$ and $m_{y,n}$ are, respectively, the x and y components of the transverse magnetization of the nucleus in its nth state. The time course of the vector $\mathbf{m}$ can be obtained by solving the McConnell equation for an arbitrary number of exchanging states[21]

$$\frac{\mathrm{d}}{\mathrm{d}t}\mathbf{m} = (\mathbf{K} - \mathbf{R} + i\mathbf{W})\mathbf{m} \tag{2}$$

in which $\mathbf{K}$ is the kinetic matrix for chemical exchange; $\mathbf{R}$ is the relaxation matrix, a diagonal matrix with diagonal elements R_{nn} that represent the transverse relaxation rate for the nth state; and $\mathbf{W}$ is the chemical shift matrix, a diagonal matrix with diagonal elements W_{nn} given by $2\pi\delta_n$, in which δ_n represents the chemical shift in hertz for the nth state. Equation 2 describes the time evolution of the nuclear transverse magnetizations for a system involving dynamic transitions between different states and assumes that the intrinsic relaxation rates and chemical shifts of individual states are independent of the kinetics of the transitions. This assumption is valid for processes that occur on a microsecond or slower time scale.

To consider the system of protein translocation on DNA, we set the basis vector $\mathbf{m}$ for a nucleus in the protein as follows. The first element corresponds to the free state of the protein, and the other elements correspond to DNA-bound states of the protein at distinct sites on the DNA. The sites are indexed sequentially as shown in Figure 1B. The kinetic matrix $\mathbf{K}$ is composed of three matrices for the sliding ($\mathbf{K}_s$), dissociation–association ($\mathbf{K}_{da}$), and intersegment transfer ($\mathbf{K}_{it}$) processes

$$\mathbf{K} = \mathbf{K}_s + \mathbf{K}_{da} + \mathbf{K}_{it} \tag{3}$$

The explicit forms of these kinetic matrices for a system with a protein and a DNA duplex are given in Figure 1A. The matrices for a system with a protein and two DNA duplexes are given in the Supporting Information.

NMR Line Shape for Protein Undergoing Translocation on DNA. The solution of eq 2 can be obtained using the initial basis vector $\mathbf{m}(0)$ and a matrix exponential as a propagator

$$\mathbf{m}(t) = \exp\{(\mathbf{K} - \mathbf{R} + i\mathbf{W})t\}\mathbf{m}(0) \tag{4}$$

The initial basis vector requires information of the equilibrium populations of individual states. For our current discrete-state kinetic model (Figure 1A), the equilibrium concentrations can readily be obtained by solving the following simultaneous equations.

$$[\mathrm{P}]_{eq}[\mathrm{D}]_{eq}/[\mathrm{PD}]_{eq} = k_{off}/k_{on} \tag{5}$$

$$P_{tot} = [\mathrm{P}]_{eq} + \lambda[\mathrm{PD}]_{eq} \tag{6}$$

$$D_{tot} = [\mathrm{PD}]_{eq} + [\mathrm{D}]_{eq} \tag{7}$$

where P_{tot} is the total concentration of protein; D_{tot}, the total concentration of DNA; λ, the total number of sites on the DNA ($2N$ for a system with a duplex; $4N$ for a system with two duplexes); $[\mathrm{P}]_{eq}$, the equilibrium concentration of the protein in the free state; $[\mathrm{D}]_{eq}$, the equilibrium concentration of each DNA site in the free state; and $[\mathrm{PD}]_{eq}$, the equilibrium concentration of each DNA site in the protein-bound state. Equation 5 is due to the principle of the detailed balance.[23]

The sum of $\mathbf{m}(t)$ elements, $s(t) = \sum m_n(t)$, corresponds to the free induction decay of the signal from this nucleus. The NMR spectrum of this system corresponds to the real part of the Fourier transform of $s(t)$

$$A(\delta) = \mathrm{Re}\left[\int_0^\infty s(t)\exp(-2\pi i\delta t)\,\mathrm{d}t\right] \tag{8}$$

In the fast exchange regime, which is the case for the rapid translocation of a protein on nonspecific DNA,[8,10−12,24] the NMR line shape can be approximated with a Lorentzian function

$$L(\delta) = aR_{2app}/[R_{2app}^2 + 4\pi^2(\delta - \delta_{app})^2] \tag{9}$$

in which R_{2app} represents an apparent transverse relaxation rate and δ_{app} represents an apparent peak position of the NMR signal from the protein. Values of R_{2app} and δ_{app} can readily be calculated through nonlinear least-squares fitting of eq 9 for a peak in the spectrum $A(\delta)$. These analyses allow us to analyze how translocations through sliding, dissociation/reassociation, and intersegment transfer can influence the line shapes of NMR signals from a protein bound nonspecifically to DNA.

Mixture Approach. On the basis of the abovementioned theoretical framework, we assess the NMR approach that Iwahara and colleagues proposed to obtain kinetic information on the intermolecular translocation of proteins between two different DNA duplexes of the same length and similar sequences.[8,10] This approach (Figure 2A), which we refer to

DOI: 10.1021/acs.jpcb.7b07779
J. Phys. Chem. B 2017, 121, 9548−9556

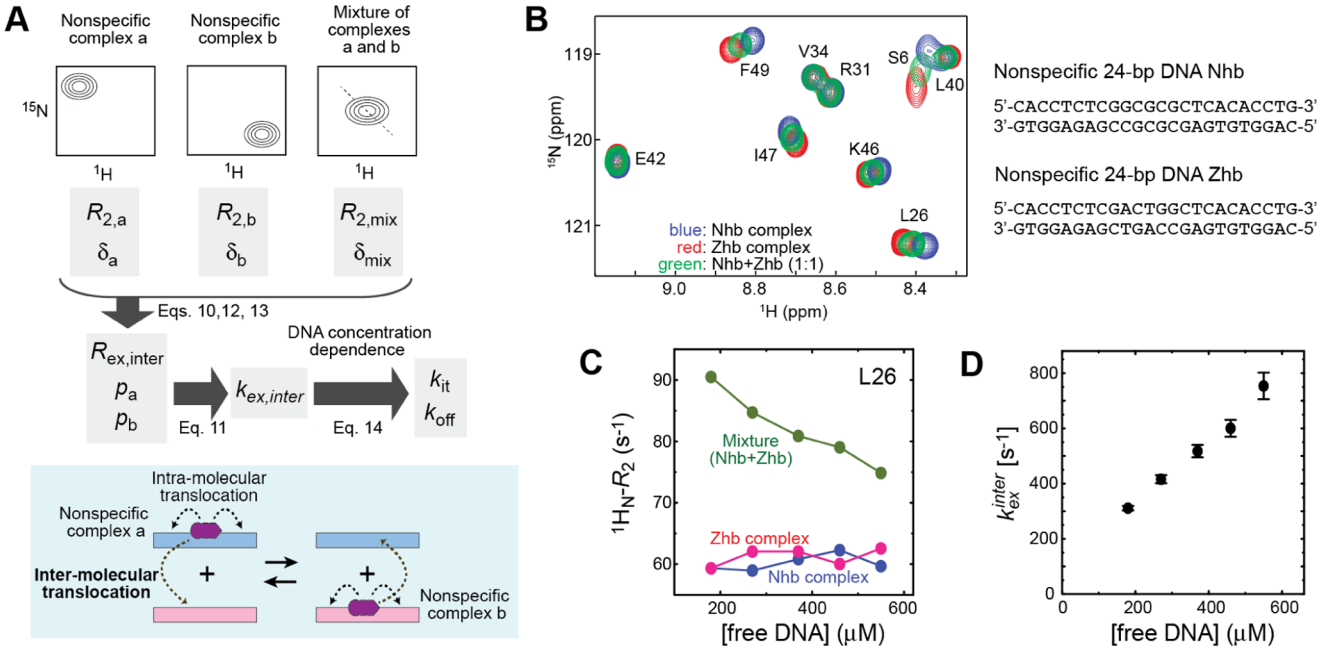

Figure 2. Mixture approach for the determination of kinetic rate constants of intermolecular translocations between two nonspecific DNA duplexes. (A) Overall scheme of the mixture approach. (B–D) Example data obtained from the mixture approach experiment for the nonspecific DNA complexes of the HoxD9 homeodomain.[8] (B) ^{1}H–^{15}N heteronuclear single-quantum coherence (HSQC) spectra measured for the nonspecific DNA complexes of the ^{2}H/^{15}N-labeled HoxD9 homeodomain. Three spectra recorded for the individual complexes (red and blue) and for their mixture (green) are overlaid. (C) Apparent ^{1}H R_2 data obtained from the Lorentzian line shape analysis of samples at various concentrations of DNA. (D) Kinetic rate constants for intermolecular translocations between the two nonspecific complexes calculated from the ^{1}H R_2 data together with eqs 10–13.

as the mixture approach, involves ^{1}H NMR line shape-based analysis for three samples of nonspecific DNA complexes of a deuterated ^{15}N-labeled protein. In this approach, protein amide ^{1}H line shapes are analyzed for three sets of ^{1}H–^{15}N spectra: two sets are of separate nonspecific complexes with DNA duplexes a and b and the other set is of a 1:1 mixture of the two nonspecific complexes. For the line shape analysis, deuterated proteins are used to avoid the splitting caused by $^{3}J_{\mathrm{HN-H}\alpha}$ coupling. Assuming that the mixture of the two nonspecific complexes can be regarded as a system with a macroscopic two-state exchange, the apparent transverse relaxation rate for the mixture is given by

$$R_{2\mathrm{app,mix}} = p_{\mathrm{a}} R_{2\mathrm{app,a}} + p_{\mathrm{b}} R_{2\mathrm{app,b}} + R_{\mathrm{ex,inter}} \quad (10)$$

where p represents a population and $R_{2\mathrm{app}}$ represents an apparent transverse relaxation rate. The third term, $R_{\mathrm{ex,inter}}$, arises from the intermolecular protein translocations between DNA duplexes a and b. When no refocusing pulses are involved, which is the case for the direct ^{1}H detection period, this exchange term may be approximated by[25]

$$R_{\mathrm{ex,inter}} = 4\pi^2 p_{\mathrm{a}} p_{\mathrm{b}} (\delta_{\mathrm{app,a}} - \delta_{\mathrm{app,b}})^2 / k_{\mathrm{ex,inter}} \quad (11)$$

where δ_{app} represents an apparent chemical shift in Hz units and $k_{\mathrm{ex,inter}}$ is the exchange rate constant for intermolecular translocations between DNA duplexes a and b. In the mixture approach, the $R_{2\mathrm{app}}$ rates and the chemical shifts (δ_{app}) are determined from the line shape analysis. When the intermolecular translocations of proteins nonspecifically bound to DNA occur in the fast exchange regime, the populations p_{a} and p_{b} are also determined from the chemical shifts

$$p_{\mathrm{a}} = (\delta_{\mathrm{app,mix}} - \delta_{\mathrm{app,b}})/(\delta_{\mathrm{app,a}} - \delta_{\mathrm{app,b}}) \quad (12)$$

$$p_{\mathrm{b}} = (\delta_{\mathrm{app,a}} - \delta_{\mathrm{app,mix}})/(\delta_{\mathrm{app,a}} - \delta_{\mathrm{app,b}}) \quad (13)$$

These experimentally determined parameters, along with eq 11, allow for the determination of the $k_{\mathrm{ex,inter}}$ constant. Some examples of actual experimental data are shown in Figure 2B–D.

By measuring this exchange rate constant $k_{\mathrm{ex,inter}}$ at some different DNA concentrations, the kinetic contributions of intersegment transfer and dissociation/reassociation mechanisms can be decomposed. When $k_{\mathrm{off}} \ll k_{\mathrm{on}}$ [free DNA], the exchange rate constant for intermolecular translocations is given by

$$k_{\mathrm{ex,inter}} = k_{\mathrm{off}} + 2Nk_{\mathrm{it}}\,[\mathrm{free\ DNA}] \quad (14)$$

in which $2Nk_{\mathrm{it}}$ corresponds to the macroscopic rate constant for intersegment transfer (derivation of this equation is described in the Supporting Information). Thus, the DNA concentration-dependent $k_{\mathrm{ex,inter}}$ data allow for the determination of k_{off} and k_{it} constants. The linear dependence on DNA concentration for the $k_{\mathrm{ex,inter}}$ data was actually observed for the HoxD9 homeodomain (Figure 2D) and the Egr-1 zinc-finger protein.[8,10]

The mixture approach adopts a simplistic approximation for a macroscopic two-state exchange, although there exist many microscopic states where proteins are located at different sites on the DNA or in the free state. Thus, the validity of this approach is not immediately obvious. Here we rigorously examine its validity.

Computation. All computations in this study were conducted with MATLAB R2016b software and its optimization toolbox (MathWorks) installed on an Apple Mac Mini.

DOI: 10.1021/acs.jpcb.7b07779
J. Phys. Chem. B 2017, 121, 9548–9556

The MATLAB function "expm" was used to calculate the matrix exponential in eq 4. The MATLAB function "nlinfit" was used for Lorentzian line shape fitting with eq 9 to calculate the $R_{2,app}$ and δ_{app} parameters from the simulated line shapes. The source codes of the MATLAB scripts for the calculations used for Figures 3 and 5 are provided in Supporting Information.

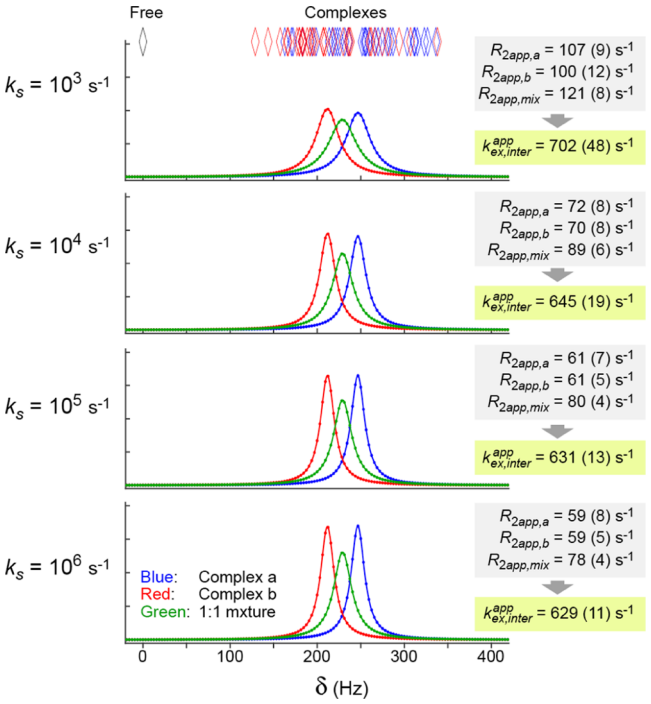

Figure 3. NMR line shapes simulated with eqs 2–8 together with the discrete-state kinetic model for a protein undergoing translocations on DNA (N = 16). The following conditions were used: P_{tot} = 200 μM, D_{tot} = 600 μM, k_{off} = 100 s^{-1}, k_{on} = 10^7 M^{-1} s^{-1}, and k_{it} = 4 × 10^4 M^{-1} s^{-1}. The intrinsic transverse relaxation rates were set to 30 s^{-1} for the free protein and 55 s^{-1} for the DNA-bound protein. The chemical shift of the free protein was set to 0 Hz, and the chemical shifts of 32 DNA-bound states of the protein for each DNA duplex were randomly generated (indicated with diamond-shaped symbols) with a standard deviation of 50 Hz and a mean of $\bar{\delta}_a$ = 250 Hz (complex a) or $\bar{\delta}_b$ = 215 Hz (complex b). The shown spectra were simulated with four different sliding rate constants k_s = 10^3, 10^4, 10^5, and 10^6 s^{-1}. The apparent exchange rates $k^{app}_{ex,inter}$ for intermolecular translocations were calculated from the $R_{2app,a}$, $R_{2app,b}$, and $R_{2app,mix}$ rates and the apparent chemical shifts using eqs 10–13. The true $k_{ex,inter}$ constant (given by eq 14) is 612 s^{-1} for these cases. Numbers in parentheses are standard deviations for the calculations with 100 different sets of chemical shifts.

Kinetic Parameters in the Simulations. Conditions similar to those of the systems of the nonspecific complexes of 24 bp DNA and the HoxD9 homeodomain[8] were used for the simulations with eqs 2–8. Each DNA duplex was treated as having 16 sites (N = 16) (see Figure 1B). For the current discrete-state model (Figure 1A), the macroscopic apparent dissociation constant $K_{d,app}$ for the nonspecific DNA complex corresponds to $k_{off}/(2Nk_{on})$. In all simulations, the rate constants k_{on} and k_{off} were chosen to satisfy k_{off}/k_{on} = 10^{-5} M, which gives a value of $K_{d,app}$ comparable to the value obtained experimentally for the nonspecific DNA complexes of the HoxD9 homeodomain (0.3 μM at 20 mM NaCl).[8]

To cover a realistic possible range, the sliding rate constant k_s was set to values on the order of 10^3–10^6 s^{-1}. This choice was based on previously known one-dimensional diffusion coefficients D_1 for the sliding of proteins on DNA. As mentioned above, D_1 in bp^2 s^{-1} units is equivalent to k_s in s^{-1} units. D_1 is often given in μm^2 s^{-1}, which can be obtained from a value in bp^2 s^{-1} by multiplying the latter by 1.16 × 10^{-7}. Previous biophysical or biochemical studies showed that D_1 is typically on the order of 10^4–10^6 bp^2 s^{-1} (e.g., see refs9, 20, 26–29).

The macroscopic intersegment transfer rate constant (corresponding to $2Nk_{it}$) for the HoxD9 homeodomain was observed to be 1.4 × 10^6 M^{-1} s^{-1} for a system of N = 16,[8] which corresponds to k_{it} = 4.4 × 10^4 M^{-1} s^{-1}. For Figures 3 and 5, the k_{it} constant was set near this value (see the captions). For more general assessment in Figure 4, the intersegment transfer rate constant k_{it} was set to values on the order of 10^3–10^6 M^{-1} s^{-1} to adequately cover a realistic range.[8−10,19,20,30]

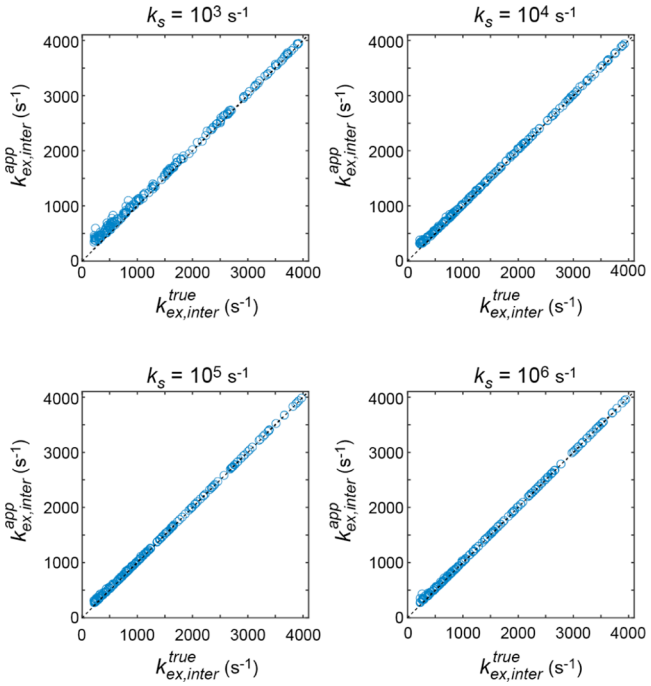

Figure 4. Accuracy assessment for the mixture approach. Each graph compares the apparent ($k^{app}_{ex,inter}$) and true ($k^{true}_{ex,inter}$) exchange rate constants for protein translocations between two DNA duplexes. The $k^{app}_{ex,inter}$ constants are those obtained from the simulated NMR line shapes using eqs 9–13. The $k^{true}_{ex,inter}$ constants are those calculated from the k_{off} and k_{it} constants using eq 14. The following conditions were used for the simulations: P_{tot} = 200 μM, D_{tot} = 600 μM, and k_{off}/k_{on} = 10^{-5} M (the apparent affinity equals this value divided by 2N); k_s = 10^3, 10^4, 10^5, and 10^6 s^{-1} were used. The values of k_{off} were randomly chosen between 1 and 10^3 s^{-1} and those of k_{it} were randomly chosen between 10^3 and 10^6 M^{-1} s^{-1}, satisfying $2\pi|\bar{\delta}_a - \bar{\delta}_b| < k^{true}_{ex,inter} < 4000$ s^{-1} (see the main text). The results of 200 calculations are shown for each panel.

NMR Parameters in the Simulations. In the NMR line shape simulations, the chemical shift of the free protein was set to 0 Hz. Each of the DNA duplexes a and b yields 32 (=2N) states of the DNA-bound protein. The chemical shifts of the individual states of the DNA-bound protein were randomly chosen from Gaussian distributions with a standard deviation and a mean, as indicated in the figure captions. The apparent chemical shift differences between two different nonspecific DNA complexes, $|\bar{\delta}_a - \bar{\delta}_b|$, were chosen on the basis of typical range of chemical shift differences between two different nonspecific DNA complexes (see Figure 2B). The standard

DOI: 10.1021/acs.jpcb.7b07779
J. Phys. Chem. B 2017, 121, 9548–9556

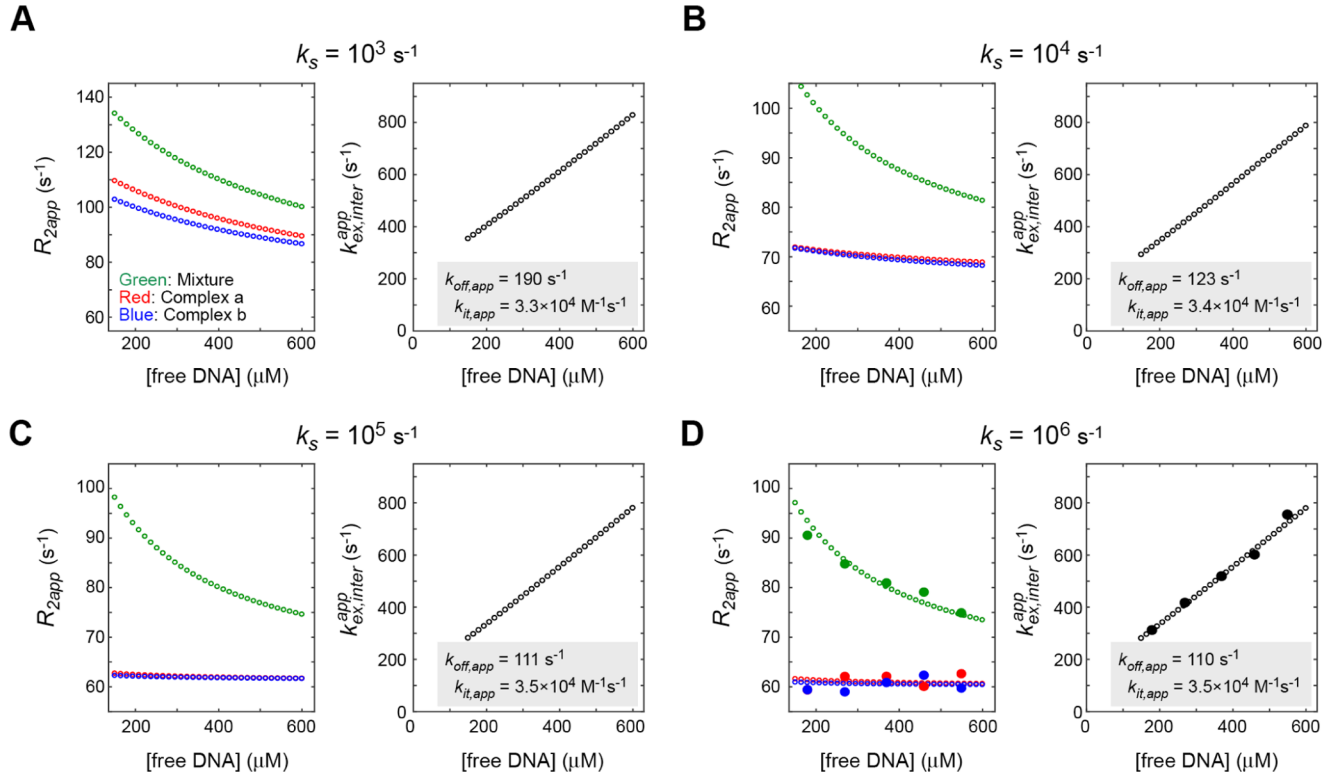

Figure 5. (A–D) Simulations of the DNA concentration dependence of the line shape-based R_2 relaxation rates and the exchange rates $k_{ex,inter}$ for the intermolecular translocations of proteins between two DNA duplexes (both with N = 16). Apparent k_{off} and k_{it} constants calculated from the simulated DNA concentration-dependent $k_{ex,inter}$ data are also indicated. The following conditions were used for the simulations: P_{tot} = 200 μM, k_{off} = 80 s^{-1}, k_{on} = 0.8 × 10^7 M^{-1} s^{-1}, k_{it} = 3.6 × 10^4 M^{-1} s^{-1}, and k_s = 10^3, 10^4, 10^5, and 10^6 s^{-1}. For each complex, the chemical shifts of 32 DNA-bound states of the protein were randomly generated with a standard deviation of 35 Hz and a mean of $\bar{\delta}_a$ =250 Hz (Complex a) or $\bar{\delta}_b$ = 218 Hz (complex b). Intrinsic transverse relaxation rates were set to 60 s^{-1} for the complexes. These parameters were chosen to reproduce the experimental data for the nonspecific DNA complexes of the HoxD9 homeodomain (Figure 2). In Panel D, experimental data (large circles) are also shown together with the simulated data (small circles).

deviation of true chemical shifts of individual DNA-bound states is difficult to assess but was set to 35–50 Hz in the simulations; it was assumed that this deviation is comparable to $|\bar{\delta}_a - \bar{\delta}_b|$. The intrinsic transverse relaxation rates for the free and DNA-bound states were chosen on the basis of experimental data for the DNA complex and the free protein of the HoxD9 homeodomain.[31,32] In the simulations, the first element of the initial basis vector $\mathbf{m}(0)$ for the McConnell equation was set to $[P]_{eq}/P_{tot}$ and the other elements were set to $[PD]_{eq}/P_{tot}$.

RESULTS AND DISCUSSION

Through simulations using numerical solutions of the McConnell equation incorporating the discrete-state kinetics model, we assessed how the sliding, dissociation/association, and intersegment transfer affect NMR signals from proteins interacting nonspecifically with DNA.

Protein NMR Line Shape for Nonspecific DNA Complexes. Using eqs 2–8, we simulated the NMR line shapes of signals from a protein that changes its location through nonspecific interactions with DNA (N = 16). Figure 3 shows some examples of NMR line shapes that were simulated for two nonspecific DNA complexes a and b (blue and red, respectively) and their 1:1 mixture (green). For each case, the total concentrations of protein and DNA are set at P_{tot} = 200 μM and D_{tot} = 600 μM, respectively. In Figure 3, the kinetic rate constants are set as follows: the association rate constant k_{on} = 10^7 M^{-1} s^{-1}, the dissociation rate constant k_{off} = 100 s^{-1}, the rate constant for intersegment transfer k_{it} = 4 × 10^4 M^{-1} s^{-1}, and the rate constant for sliding k_s = 10^3, 10^4, 10^5, and 10^6 s^{-1}. The population of the free protein is calculated to be only 0.053% under these conditions. The chemical shifts of the individual states are shown with diamond-shaped symbols in Figure 3. Although the systems involve 33 (=1 + 2 × 16) or 65 (=1 + 2 × 2 × 16) different states, each system showed only a single signal due to the rapid translocations in the fast exchange regime.

Through nonlinear least-squares fitting with eq 9, the apparent transverse relaxation rates were calculated from the simulated line shapes. The Lorentzian function given by eq 9 gave excellent fit for the simulated line shapes in the fast exchange regime. When the sliding process is relatively slow (e.g., k_s = 10^3 and 10^4 s^{-1}), the NMR line shape was broader, and the apparent transverse relaxation rates of individual complexes ($R_{2app,a}$ and $R_{2app,b}$) were considerably larger than the intrinsic transverse relaxation rate for the DNA-bound protein (i.e., 55 s^{-1}). When the sliding is fast (k_s = 10^6 s^{-1}), the apparent transverse relaxation rates were only slightly larger (by <10%) than the intrinsic transverse relaxation rate. For all simulations, the apparent transverse relaxation rate for the mixture ($R_{2app,mix}$) was significantly larger than $R_{2,app,a}$ and $R_{2app,b}$. In Figure 3, this is also evident from the shortest peak height for the signal simulated for the mixture. The faster apparent transverse relaxation for the mixture is due to an

DOI: 10.1021/acs.jpcb.7b07779
J. Phys. Chem. B 2017, 121, 9548–9556

additional exchange contribution arising from intermolecular translocations of the protein between the two nonspecific DNA duplexes a and b, for which apparent chemical shifts are different.

Validation of the Mixture Approach. Using the apparent transverse relaxation rates $R_{2app,a}$, $R_{2app,b}$, and $R_{2app,mix}$ from the simulated NMR line shapes, the apparent exchange rate constant $k_{ex,inter}$ for the intermolecular translocations of protein between two nonspecific DNA duplexes was calculated using eqs 10−13. This corresponds to the "apparent" $k_{ex,inter}$ constant from the mixture approach experiment in silico. Unlike any real experiment, we know the "true" $k_{ex,inter}$ constant given by eq 14 for the simulation data. By comparing the apparent and true values of $k_{ex,inter}$ constants from the simulations under various conditions, we assessed the accuracy of the mixture approach.

For this assessment, we ran simulations with N = 16, P_{tot} = 200 μM, D_{tot} = 600 μM, k_{off}/k_{on} = 10^{-5} M, and k_s = 10^3, 10^4, 10^5, and 10^6 s^{-1}. The values of k_{off} and k_{it} were randomly chosen in the ranges of 1−10^3 s^{-1} and 10^3−10^6 M^{-1} s^{-1}, respectively, but only those values satisfying $2\pi|\bar{\delta}_a - \bar{\delta}_b| < k^{true}_{ex,inter} < 4000$ s^{-1} were used. The first inequality is due to being in the fast exchange regime, whereas the second inequality is due to the fact that $k^{true}_{ex,inter} \geq 4000$ s^{-1} is practically difficult to determine with the line shape analysis. For each set, the chemical shifts of 32 individual states of the complexes a and b were also randomly chosen from Gaussian distributions with $\bar{\delta}_a$ = 250 Hz and $\bar{\delta}_b$ = 215 Hz and a standard deviation of 50 Hz. Figure 4 shows correlation plots that compare the true and apparent $k_{ex,inter}$ constants. The apparent $k_{ex,inter}$ constants were in good agreement with the true values, especially when sliding is fast. When sliding is relatively slow (k_s = 10^3 s^{-1}), the apparent $k_{ex,inter}$ constant was systematically larger than the true value by 10−20% when $k_{ex,inter}$ < 1000 s^{-1}. These results show that despite the use of the simplistic two-state approximation (eqs 10−13) for systems with a larger number of microscopic states, the mixture approach provides accurate kinetic information about the intermolecular translocations of protein between two DNA duplexes.

DNA Concentration Dependence. Using the line shape simulations with the discrete-state kinetic model, we also assessed the accuracy of the mixture approach in the determination of k_{off} and k_{it} from DNA concentration dependence data. Figure 5 shows the DNA concentration dependence of the apparent transverse relaxation rates R_{2app} for the individual complexes and their mixture and the apparent $k_{ex,inter}$ constants calculated from the apparent transverse relaxation rates. These correspond to the simulations for the experimental data shown in Figure 2C,D. As observed in the experiment, the simulations showed that the apparent exchange rate $k_{ex,inter}$ linearly depends on the concentration of free DNA (Figure 5). According to eq 14, the slope of this concentration dependence corresponds to $2Nk_{it}$ and the intercept at the vertical axis corresponds to k_{off}. Using this equation together with the concentration-dependent $k_{ex,inter}$ data from the NMR simulations, we calculated the apparent k_{off} and k_{it} constants (shown in the insets of Figure 5). We found that the apparent k_{off} constant from the DNA concentration-dependent $k_{ex,inter}$ data is reasonably accurate when the sliding occurs with a realistic rate constant (k_s = 10^4−10^6 s^{-1}), although the k_{off} constant tends to be overestimated when the sliding is slower. We also found that the apparent intersegment transfer rate constant k_{it} from this analysis is in excellent agreement with the true value regardless of the sliding rate constant k_s used in the simulations. Relatively low accuracy for the $k_{off,app}$ constant can be explained as follows. When sliding is relatively slow, the $k^{app}_{ex,inter}$ rate is overestimated, as seen in Figures 3 and 4. Because both sliding and dissociation are first-order processes (i.e., independent of the DNA concentration) and the $k_{off,app}$ constant is determined as the DNA concentration-independent term in eq 14, this inflation of $k^{app}_{ex,inter}$ due to slow sliding affects $k_{off,app}$ to a larger degree. Nonetheless, these simulations suggest that the mixture approach allows for reasonably accurate kinetic analysis of intermolecular protein translocations between two DNA duplexes.

Impact of Sliding. Interestingly, our simulations also indicate that the DNA concentration dependence of the apparent transverse relaxation rates can provide qualitative information on sliding. This is clearly seen in Figure 5. When the sliding is relatively slow (e.g., k_s = 10^3−10^4 s^{-1}), the R_{2app} rates for individual complexes depend strongly on the DNA concentration. In contrast, when the sliding is relative fast (e.g., k_s = 10^5−10^6 s^{-1}), the $R_{2app,a}$ and $R_{2app,b}$ rates are virtually independent of the DNA concentration. This observation can be qualitatively explained as follows. Exchange between two particular DNA-bound states could occur through sliding or intermolecular translocation between two DNAs of the same species (e.g., DNA a to a′ or b to b′). The kinetics of the sliding, which is a first-order process, does not depend on DNA concentration, whereas the intermolecular translocation does depend on DNA concentration (see eq 14). When the exchange through sliding is much faster than the exchange through intermolecular translocation, the exchange term within the apparent relaxation rates $R_{2app,a}$ and $R_{2app,b}$ becomes negligible, and these relaxation rates become close to the intrinsic R_2 rate. However, when the time scales of these two translocation mechanisms are comparable, changes in DNA concentration can alter the overall exchange rate, causing $R_{2app,a}$ and $R_{2app,b}$ to depend on the concentration of DNA.

In the case of the experimental data shown in Figure 2C, the R_{2app} rates for the individual nonspecific complexes of the HoxD9 homeodomain appear to be virtually independent of the free DNA concentration. The lack of DNA concentration dependence of these R_{2app} rates suggests that the one-dimensional diffusion coefficient D_1 for sliding of the HoxD9 homeodomain is on the order of 10^5−10^6 bp^2 s^{-1}. This estimate is consistent with typical D_1 values determined by fluorescence methods for other relatively small proteins.[9,20,33]

The computational data shown in Figure 5 correspond to the experimental results for the nonspecific complexes of the HoxD9 homeodomain shown in Figure 2C,D. Through manual adjustment of the simulation parameters (see Figure 5 caption), we were able to reproduce the DNA concentration dependence of $R_{2app,a}$, $R_{2app,b}$, $R_{2app,mix}$, and $k^{app}_{ex,inter}$ data, as shown in Figure 5D. At this point, however, this model cannot be directly used to determine the kinetic parameters because the calculations require chemical shifts of individual states. Nonetheless, the good agreement between the simulations and experimental data supports validity of the discrete-state kinetic model used in the current study.

Practical Guidelines for the Mixture Approach. Our simulations based on discrete-state kinetic model show that the mixture approach based on eqs 10−14 can provide accurate kinetic information on protein translocation on DNA. This approach is applicable only for translocation of proteins between two different DNA duplexes occurring in a fast exchange regime. This requirement is likely satisfied for

DOI: 10.1021/acs.jpcb.7b07779
J. Phys. Chem. B 2017, 121, 9548−9556

nonspecific DNA duplexes on which proteins can rapidly slide.[8,10,19,20] By overlaying three $^{1}H-^{15}N$ HSQC spectra recorded for the individual complexes and their mixture (as shown in Figure 2B), one can tell whether or not the translocations occur in a fast exchange regime. In the fast exchange regime, the mixture sample should exhibit a single set of the $^{1}H-^{15}N$ correlation signals in the population-averaged positions. When the translocations occur in an intermediate exchange regime, line shapes significantly deviate from Lorentzian shapes (examples shown in the Supporting Information). In the slow exchange regime, the mixture should exhibit two different sets of signals. For example, if the two DNA duplexes contain high-affinity sites for the protein, its translocation between the two duplexes can occur in a slow exchange regime. In such a case, $^{15}N_z$ exchange spectroscopy[34−36] can be used to study the translocation kinetics, as previously demonstrated for some specific protein−DNA complexes.[30,36,37] If the translocations occur too slowly for exchange spectroscopy, nonequilibrium real-time kinetics approach can be used.[38]

Potential Expansion for Other NMR Methods. Although our current study utilizes the discrete-state kinetics model for protein translocation on DNA (Figure 1A) only for the NMR line shape analysis, this kinetics model can readily be implemented into the matrix-based equations for the Carr−Purcell−Meiboom−Gill scheme, as described by Allerhand and Thiele.[21] Equations for some other NMR methods on chemical exchange also deal with a kinetic matrix. Our discrete-state kinetics model for protein translocation on DNA can be directly incorporated into such equations: for example, those for paramagnetic relaxation enhancement,[39] $R_{1\rho}$ relaxation,[40] or cross saturation.[41] Thus, the current approach with the discrete-state kinetic model could potentially help explore investigations of protein translocation on DNA using these NMR methods as well.

CONCLUSIONS

In this article, we demonstrated the use of the discrete-state kinetics model together with the McConnell equation for NMR-based analysis of protein translocation on DNA. The simulations using this model were used to validate the mixture approach for analyzing the kinetics of intermolecular translocations of a protein between two nonspecific DNA duplexes in the fast exchange regime. Although the mixture approach adopts a simplistic two-state model, our numerical simulations with the more rigorous model accounting for the sliding, hopping, and intersegment transfer suggest that the mixture approach yields accurate kinetic information on rapid intermolecular translocations between two nonspecific DNA duplexes. Although the mixture approach does not provide quantitative information on intramolecular translocation, our simulations suggest that the DNA concentration dependence data can give at least qualitative information about the one-dimensional diffusion coefficient for sliding. The discrete-state kinetics model can readily be incorporated into the equations for other NMR methods. Therefore, protein translocation on DNA can be studied using this kinetic model in conjunction with some different NMR methods that can deal with fast exchange. Such investigations would allow us to better understand how proteins scan DNA.

ASSOCIATED CONTENT

Supporting Information

The Supporting Information is available free of charge on the ACS Publications website at DOI: 10.1021/acs.jpcb.7b07779.

Kinetic matrices for a system with a protein and two nonspecific DNA duplexes; examples of non-Lorentzian line shapes when protein translocation on DNA is slow; derivation of eq 14; MATLAB scripts and data files used for Figures 3 and 5 (PDF)

AUTHOR INFORMATION

Corresponding Author

*E-mail: j.iwahara@utmb.edu.

ORCID

Junji Iwahara: 0000-0003-4732-2173

Notes

The authors declare no competing financial interest.

ACKNOWLEDGMENTS

This work was supported by Grant R01-GM107590 from the National Institutes of Health (to J.I.) and Grant CHE-1608866 from the National Science Foundation (to J.I.).

REFERENCES

(1) von Hippel, P. H.; Berg, O. G. Facilitated target location in biological systems. *J. Biol. Chem.* **1989**, *264*, 675−678.

(2) Halford, S. E.; Marko, J. F. How do site-specific DNA-binding proteins find their targets? *Nucleic Acids Res.* **2004**, *32*, 3040−3052.

(3) Mirny, L.; Slutsky, M.; Wunderlich, Z.; Tafvizi, A.; Leith, J.; Kosmrlj, A. How a protein searches for its site on DNA: the mechanism of facilitated diffusion. *J. Phys. A: Math. Theor.* **2009**, *42*, No. 434013.

(4) Kolomeisky, A. B. Physics of protein−DNA interactions: mechanisms of facilitated target search. *Phys. Chem. Chem. Phys.* **2011**, *13*, 2088−2095.

(5) Tafvizi, A.; Mirny, L. A.; van Oijen, A. M. Dancing on DNA: kinetic aspects of search processes on DNA. *ChemPhysChem* **2011**, *12*, 1481−1489.

(6) Clore, G. M. Exploring translocation of proteins on DNA by NMR. *J. Biomol. NMR* **2011**, *51*, 209−219.

(7) Kalodimos, C. G.; Biris, N.; Bonvin, A. M. J. J.; Levandoski, M. M.; Guennuegues, M.; Boelens, R.; Kaptein, R. Structure and flexibility adaptation in nonspecific and specific protein−DNA complexes. *Science* **2004**, *305*, 386−389.

(8) Iwahara, J.; Zweckstetter, M.; Clore, G. M. NMR structural and kinetic characterization of a homeodomain diffusing and hopping on nonspecific DNA. *Proc. Natl. Acad. Sci. U.S.A.* **2006**, *103*, 15062−15067.

(9) Zandarashvili, L.; Esadze, A.; Vuzman, D.; Kemme, C. A.; Levy, Y.; Iwahara, J. Balancing between affinity and speed in target DNA search by zinc-finger proteins via modulation of dynamic conformational ensemble. *Proc. Natl. Acad. Sci. U.S.A.* **2015**, *112*, E5142−E5149.

(10) Zandarashvili, L.; Vuzman, D.; Esadze, A.; Takayama, Y.; Sahu, D.; Levy, Y.; Iwahara, J. Asymmetrical roles of zinc fingers in dynamic DNA-scanning process by the inducible transcription factor Egr-1. *Proc. Natl. Acad. Sci. U.S.A.* **2012**, *109*, E1724−E1732.

(11) Vandevenne, M.; Jacques, D. A.; Artuz, C.; Nguyen, C. D.; Kwan, A. H. Y.; Segal, D. J.; Matthews, J. M.; Crossley, M.; Guss, J. M.; Mackay, J. P. New insights into DNA recognition by zinc fingers revealed by structural analysis of the oncoprotein ZNF217. *J. Biol. Chem.* **2013**, *288*, 10616−10627.

(12) De, S.; Chan, A. C. K.; Coyne, H. J., III; Bhachech, N.; Hermsdorf, U.; Okon, M.; Murphy, M. E. P.; Graves, B. J.; McIntosh, L. P. Steric mechanism of auto-inhibitory regulation of specific and

DOI: 10.1021/acs.jpcb.7b07779
J. Phys. Chem. B 2017, 121, 9548−9556

non-specific DNA binding by the ETS transcriptional repressor ETV6. *J. Mol. Biol.* **2014**, *426*, 1390−1406.
(13) Desjardins, G.; Okon, M.; Graves, B. J.; McIntosh, L. P. Conformational dynamics and the binding of specific and nonspecific DNA by the autoinhibited transcription factor Ets-1. *Biochemistry* **2016**, *55*, 4105−4118.
(14) Loth, K.; Gnida, M.; Romanuka, J.; Kaptein, R.; Boelens, R. Sliding and target location of DNA-binding proteins: an NMR view of the lac repressor system. *J. Biomol. NMR* **2013**, *56*, 41−49.
(15) Berg, O. G.; Winter, R. B.; Von Hippel, P. H. Diffusion-driven mechanisms of protein translocation on nucleic acids. 1. Models and theory. *Biochemistry* **1981**, *20*, 6929−6948.
(16) Slutsky, M.; Mirny, L. A. Kinetics of Protein−DNA Interaction: Facilitated Target Location in Sequence-Dependent Potential. *Biophys. J.* **2004**, *87*, 4021−4035.
(17) Veksler, A.; Kolomeisky, A. B. Speed-selectivity paradox in the protein search for targets on DNA: Is it real or not? *J. Phys. Chem. B* **2013**, *117*, 12695−12701.
(18) Zhou, H.-X. Rapid search for specific sites on DNA through conformational switch of nonspecifically bound proteins. *Proc. Natl. Acad. Sci. U.S.A.* **2011**, *108*, 8651−8656.
(19) Esadze, A.; Iwahara, J. Stopped-flow fluorescence kinetic study of protein sliding and intersegment transfer in the target DNA search process. *J. Mol. Biol.* **2014**, *426*, 230−244.
(20) Esadze, A.; Kemme, C. A.; Kolomeisky, A. B.; Iwahara, J. Positive and negative impacts of nonspecific sites during target location by a sequence-specific DNA-binding protein: origin of the optimal search at physiological ionic strength. *Nucleic Acids Res.* **2014**, *42*, 7039−7046.
(21) Allerhand, A.; Thiele, E. Analysis of Carr−Purcell spin-echo NMR experiments on multiple-spin systems. II. The effect of chemical exchange. *J. Chem. Phys.* **1966**, *45*, 902−916.
(22) McConnell, H. M. Reaction rates by nuclear magnetic resonance. *J. Chem. Phys.* **1958**, *28*, 430−431.
(23) Hammes, G. G. *Thermodynamics and Kinetics for the Biological Sciences*, 3rd ed.; Wiley-Interscience: New York, 2000.
(24) Iwahara, J.; Schwieters, C. D.; Clore, G. M. Characterization of nonspecific protein−DNA interactions by ^{1}H paramagnetic relaxation enhancement. *J. Am. Chem. Soc.* **2004**, *126*, 12800−12808.
(25) Reuben, J.; Fiat, D. Nuclear magnetic resonance studies of solutions of the rare-earth ions and their complexes. IV. Concentration and temperature dependence of the oxygen-17 transverse relaxation in aqueous solutions. *J. Chem. Phys.* **1969**, *51*, 4918−4927.
(26) Bonnet, I.; Biebricher, A.; Porté, P.-L.; Loverdo, C.; Bénichou, O.; Voituriez, R.; Escudé, C.; Wende, W.; Pingoud, A.; Desbiolles, P. Sliding and jumping of single *Eco*RV restriction enzymes on non-cognate DNA. *Nucleic Acids Res.* **2008**, *36*, 4118−4127.
(27) Gorman, J.; Wang, F.; Redding, S.; Plys, A. J.; Fazio, T.; Wind, S.; Alani, E. E.; Greene, E. C. Single-molecule imaging reveals target-search mechanisms during DNA mismatch repair. *Proc. Natl. Acad. Sci. U.S.A.* **2012**, *109*, E3074−E3083.
(28) Rau, D. C.; Sidorova, N. Y. Diffusion of the restriction nuclease *Eco*RI along DNA. *J. Mol. Biol.* **2010**, *395*, 408−416.
(29) Tafvizi, A.; Huang, F.; Leith, J. S.; Fersht, A. R.; Mirny, L. A.; van Oijen, A. M. Tumor suppressor p53 slides on DNA with low friction and high stability. *Biophys. J.* **2008**, *95*, L01−L03.
(30) Iwahara, J.; Clore, G. M. Direct observation of enhanced translocation of a homeodomain between DNA cognate sites by NMR exchange spectroscopy. *J. Am. Chem. Soc.* **2006**, *128*, 404−405.
(31) Iwahara, J.; Clore, G. M. Detecting transient intermediates in macromolecular binding by paramagnetic NMR. *Nature* **2006**, *440*, 1227−1230.
(32) Iwahara, J.; Jung, Y.-S.; Clore, G. M. Heteronuclear NMR spectroscopy for lysine NH_3 groups in proteins: unique effect of water exchange on ^{15}N transverse relaxation. *J. Am. Chem. Soc.* **2007**, *129*, 2971−2980.
(33) Blainey, P. C.; van Oijen, A. M.; Banerjee, A.; Verdine, G. L.; Xie, X. S. A base-excision DNA-repair protein finds intrahelical lesion bases by fast sliding in contact with DNA. *Proc. Natl. Acad. Sci. U.S.A.* **2006**, *103*, 5752−5757.
(34) Farrow, N. A.; Zhang, O.; Forman-Kay, J. D.; Kay, L. E. A heteronuclear correlation experiment for simultaneous determination of ^{15}N longitudinal decay and chemical exchange rates of systems in slow equilibrium. *J. Biomol. NMR* **1994**, *4*, 727−734.
(35) Li, Y.; Palmer, A. G., III TROSY-selected ZZ-exchange experiment for characterizing slow chemical exchange in large proteins. *J. Biomol. NMR* **2009**, *45*, 357−360.
(36) Sahu, D.; Clore, G. M.; Iwahara, J. TROSY-based z-exchange spectroscopy: Application to the determination of the activation energy for intermolecular protein translocation between specific sites on different DNA molecules. *J. Am. Chem. Soc.* **2007**, *129*, 13232−13237.
(37) Doucleff, M.; Clore, G. M. Global jumping and domain-specific intersegment transfer between DNA cognate sites of the multidomain transcription factor Oct-1. *Proc. Natl. Acad. Sci. U.S.A.* **2008**, *105*, 13871−13876.
(38) Takayama, Y.; Sahu, D.; Iwahara, J. NMR studies of translocation of the Zif268 protein between its target DNA sites. *Biochemistry* **2010**, *49*, 7998−8005.
(39) Clore, G. M.; Iwahara, J. Theory, practice, and applications of paramagnetic relaxation enhancement for the characterization of transient low-population states of biological macromolecules and their complexes. *Chem. Rev.* **2009**, *109*, 4108−4139.
(40) Koss, H.; Rance, M.; Palmer, A. G., III General expressions for $R_{1\rho}$ relaxation for N-site chemical exchange and the special case of linear chains. *J. Magn. Reson.* **2017**, *274*, 36−45.
(41) Ueda, T.; Takeuchi, K.; Nishida, N.; Stampoulis, P.; Kofuku, Y.; Osawa, M.; Shimada, I. Cross-saturation and transferred cross-saturation experiments. *Q. Rev. Biophys.* **2014**, *47*, 143−187.

DOI: 10.1021/acs.jpcb.7b07779
J. Phys. Chem. B 2017, 121, 9548−9556